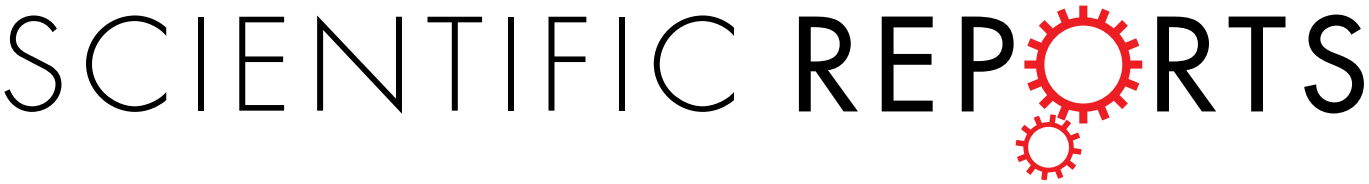

OPEN

Evolution of T Cell Responses during Measles Virus Infection and RNA Clearance

Received: 24 March 2017
Accepted: 17 August 2017
Published online: 13 September 2017

Ashley N. Nelson[1], Nicole Putnam[1,3], Debra Hauer[1], Victoria K. Baxter[1,2,4], Robert J. Adams[2] & Diane E. Griffin[1]

Measles is an acute viral disease associated both with immune suppression and development of life-long immunity. Clearance of measles virus (MeV) involves rapid elimination of infectious virus during the rash followed by slow elimination of viral RNA. To characterize cellular immune responses during recovery, we analyzed the appearance, specificity and function of MeV-specific T cells for 6 months after respiratory infection of rhesus macaques with wild type MeV. IFN-γ and IL-17-producing cells specific for the hemagglutinin and nucleocapsid proteins appeared in circulation in multiple waves approximately 2-3, 8 and 18–24 weeks after infection. IFN-γ-secreting cells were most abundant early and IL-17-secreting cells late. Both CD4$^+$ and CD8$^+$ T cells were sources of IFN-γ and IL-17, and IL-17-producing cells expressed RORγt. Therefore, the cellular immune response evolves during MeV clearance to produce functionally distinct subsets of MeV-specific CD4$^+$ and CD8$^+$ T cells at different times after infection.

Measles is a highly contagious viral disease that remains an important cause of childhood morbidity and mortality[1] with most deaths due to secondary infections[2,3]. Measles virus (MeV), the causative agent of measles, is transmitted by the respiratory route and has an incubation period of 10–14 days. From the respiratory tract, MeV spreads to local lymphatic tissue and then to multiple organs including the skin. The prodrome of fever, cough and conjunctivitis is followed by a maculopapular rash associated with development of the adaptive immune response and T cell infiltration into sites of MeV-infected skin cells[4]. Although infectious MeV is cleared soon after the appearance of the rash, MeV RNA persists in peripheral blood mononuclear cells (PBMCs), urine and nasopharyngeal secretions of both naturally infected children[5,6] and experimentally infected rhesus macaques[7] for several months.

The host adaptive immune response is necessary for control and clearance of virus[8,9] and both MeV-specific antibody and T cells contribute to gradual clearance of viral RNA from PBMCs[7]. Studies of both humans and monkeys suggest that CD8$^+$ T cells are important for clearance of infectious virus during the rash. MeV-specific cytotoxic T lymphocytes appear in blood during natural infection[10] and experimentally infected macaques depleted of CD8$^+$ T lymphocytes have viremias that are higher and of longer duration than immunologically intact monkeys[11].

Although less well studied, CD4$^+$ T lymphocytes are likely to be essential contributors to a successful immune response to MeV and establishment of life long immunity. Naïve CD4$^+$ T cells develop into functionally distinct subsets defined by the conditions required for differentiation, transcription factor expression and cytokines produced and important subtypes include Th1 cells producing interferon (IFN)-γ, Th2 cells producing IL-4, Th17 cells producing IL-17 and Treg cells producing IL-10[12]. Evaluation of cytokines in plasma of children with measles suggests that CD4$^+$ T cells predominantly produce IFN-γ during the rash period followed by a later switch to IL-4, IL-10 and IL-13 secretion as antibody production matures suggesting early development of Th1 followed by Th2 and Treg CD4$^+$ T cells[13–15]. The possible development of effector CD4$^+$ T cells producing IL-17 during the response to MeV was suggested in a vaccine study, but Th17 responses have not been systematically evaluated[16].

[1]W. Harry Feinstone Department of Molecular Microbiology and Immunology, Johns Hopkins Bloomberg School of Public Health, Johns Hopkins University School of Medicine, Baltimore, MD, 21205, USA. [2]Department of Molecular and Comparative Pathobiology, Johns Hopkins University School of Medicine, Baltimore, MD, 21205, USA. [3]Present address: Vanderbilt University School of Medicine, Nashville, TN, 37232, USA. [4]Present address: University of North Carolina School of Medicine, Chapel Hill, NC, USA. Ashley N. Nelson and Nicole Putnam contributed equally to this work. Correspondence and requests for materials should be addressed to D.E.G. (email: dgriffi6@jhu.edu)

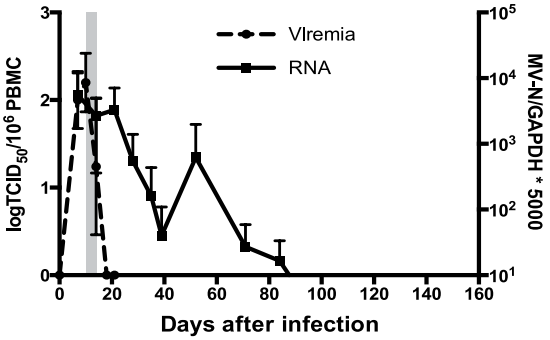

Figure 1. Measles viremia, rash and virus clearance. After intratracheal infection of rhesus macaques with the wild-type Bilthoven strain of MeV, viremia was measured by co-cultivation of serially diluted PBMCs on Vero/hSLAM cells. Data are displayed as the tissue culture infectious dose 50 ($TCID_{50}$)/10^6 PBMCs (n = 5). MeV N gene RNA in peripheral blood mononuclear cells was measured by RT-qPCR (n = 5). Gray shaded area indicates the period of the rash.

	14Y	17Y	31Y	46Y	50Y
0	–	–	–	–	–
7	–	+	–	–	+
10	+	+	+	+	+
14	+	+	+	+	+
18	–	+	+	–	+
21	–	+	–	–	+
39	–	–	–	–	–

Table 1. Presence of MeV RNA in nasal secretions.

Because it is likely that the functional evolution of T cell subsets during the prolonged phase of MeV RNA clearance is important for eventual virus clearance, immune suppression and establishment of life-long protective immunity, we characterized cellular immune responses to MeV over a period of six months after infection of rhesus macaques with a wild type strain of MeV.

Results

Measles virus RNA persists in multiple tissues. To document the time course of clearance of infectious virus and viral RNA in this cohort of 3-year old macaques, infectious virus in the blood was monitored by co-cultivation of PBMCs with Vero/hSLAM cells and viral RNA was quantified by RT-qPCR. All monkeys developed a viremia by day 7, a rash by day 10 and cleared infectious virus from PBMCs by day 18 (Fig. 1). MeV RNA was detected in respiratory secretions by 7 to 10 days after infection followed by continued shedding for 1–2 weeks (Table 1). MeV RNA in PBMCs gradually decreased after clearance of infectious virus and became undetectable 90 to 120 days after infection (Fig. 1). These data confirm that prolonged presence of viral RNA is characteristic of primary MeV infection[7].

Changes in circulating leukocytes. Numbers of total white blood cells, lymphocytes, and neutrophils in circulation were depressed during the viremia (day 10), increased and then generally were within the normal range by four weeks after infection (Fig. 2A). Both $CD8^+$ and $CD4^+$ cells were decreased from day 10–18 and then returned to baseline (Fig. 2B). There was a transient increase in the CD4:CD8 ratio as the viremia was cleared and then stabilized in the normal range (Fig. 2C).

ELISPOT analysis of IFNγ- and IL-17-secreting cells. Cells secreting IFN-γ (Fig. 3A) and IL-17 (Fig. 3C) as a result of *in vivo* activation were present at multiple times after infection with peaks at days 14–21, 52 and 126. *In vitro* MeV antigen stimulation further increased the numbers of IFN-γ-secreting cells at day 21 after infection coincident with the clearance of infectious virus and decline in viral RNA levels (Figs 1 and 3B). In contrast, peak numbers of IL-17-secreting cells in response to *in vivo* activation, as well as *in vitro* stimulation, occurred later on days 52 and 126 as viral RNA was being cleared (Figs 1 and 3D).

Both $CD4^+$ and $CD8^+$ T cells express IFN-γ during viral clearance and recovery. To determine the cellular sources and MeV protein-specific responses of early and late IFN-γ production during MeV infection, PBMCs were stimulated with overlapping H or N peptides and analyzed by multi-parameter flow cytometry. $CD4^+$ and $CD8^+$ cells specific for both H and N proteins were sources of IFN-γ throughout the course of infection (Fig. 4). $CD4^+$ T cells producing IFN-γ in response to MeV peptide stimulation were most abundant in circulation at 10 and 84 days after infection (Fig. 4A). An increase in IFN-γ^+CD8^+ T cells was observed in all

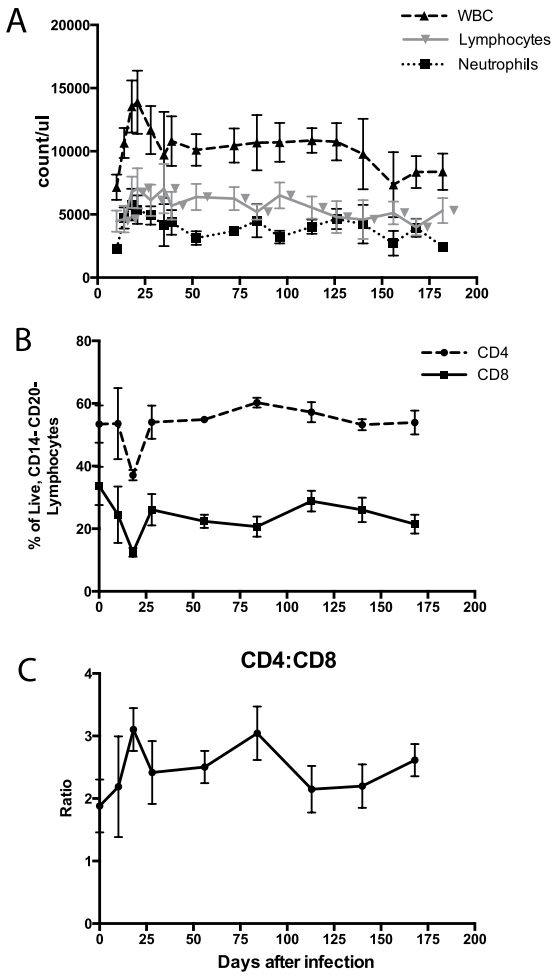

Figure 2. Changes in leukocyte counts after infection. Complete blood counts were used to measure the total numbers of circulating white blood cells (WBCs; dashed line), lymphocytes (gray line) and neutrophils (dotted line) (**A**) (n = 5). Normal ranges of cell counts for 3–4 year old rhesus macaques are: 7,700–13,000 WBCs/ml, 2,671–8,350 lymphocytes/ml, and 2,671–5,147 neutrophils/ml. Percentages of lymphocytes that were $CD4^+$ and $CD8^+$ T cells were determined by flow cytometry (**B**) and the CD4:CD8 ratio calculated (**C**) (n = 5). The normal CD4:CD8 ratio is 2.

macaques at 10 days after infection (Fig. 4B). A second wave of IFN-γ^+CD8^+ T cells appeared from 84–140 days after infection in four of the five macaques (Fig. 4B).

Several studies have suggested that the quality, as well as the magnitude of the T-cell response is important for control of virus infection[17–20]. An important measure of the functional quality of T cells is the ability to simultaneously produce multiple cytokines or polyfunctionality of these cells[17,21]. H- and N-specific $CD4^+$ and $CD8^+$ T cell polyfunctionality was assessed by measuring simultaneous expression of IFN-γ, IL-2, TNF-α ($CD4^+$ and $CD8^+$) and CD107a ($CD8^+$ only). A large fraction of H-specific $CD4^+$ T cells were polyfunctional (producing more than one cytokine) at 56 dpi (Figs 4C and 5A), while N-specific $CD4^+$ T cells were more polyfunctional at 28 dpi (Fig. 4C). In contrast, a large fraction of H- and N-specific $CD8^+$ T cells were polyfunctional at multiple time points after infection (Fig. 4D). Overall, $CD4^+$ T cells were polyfunctional primarily at earlier time points (Figs 4C and 5) while $CD8^+$ T cells were polyfunctional at both early and late phases of recovery (Figs 4D and 5). Thus, MeV infection induces prolonged multifunctional virus-specific T cell responses likely to be important for controlling and clearing infection and perhaps for induction of long-term protective immunity.

MeV-specific CD4+ and CD8+ T cells begin producing IL-17 after clearance of infectious virus. To identify and further characterize the IL-17-producing cells induced during measles, surface and intracellular cytokine staining with multicolor flow cytometry was performed with complete data available for 4 of the 5 monkeys (Fig. 6). All monkeys developed MeV-specific Th17 ($CD4^+IL\text{-}17^+$) cells (Fig. 6A). H-specific Th17 cells increased from less than 0.01% (days 0 and 10) to 1.35–2.27% of the $CD4^+$ T cell population at day 18, followed by intermittent increases above baseline throughout the follow-up period (Fig. 6A). N-specific Th17 cells were more variable. On average, Th17 H- and N- specific responses were highest on days 18 and 168 after infection.

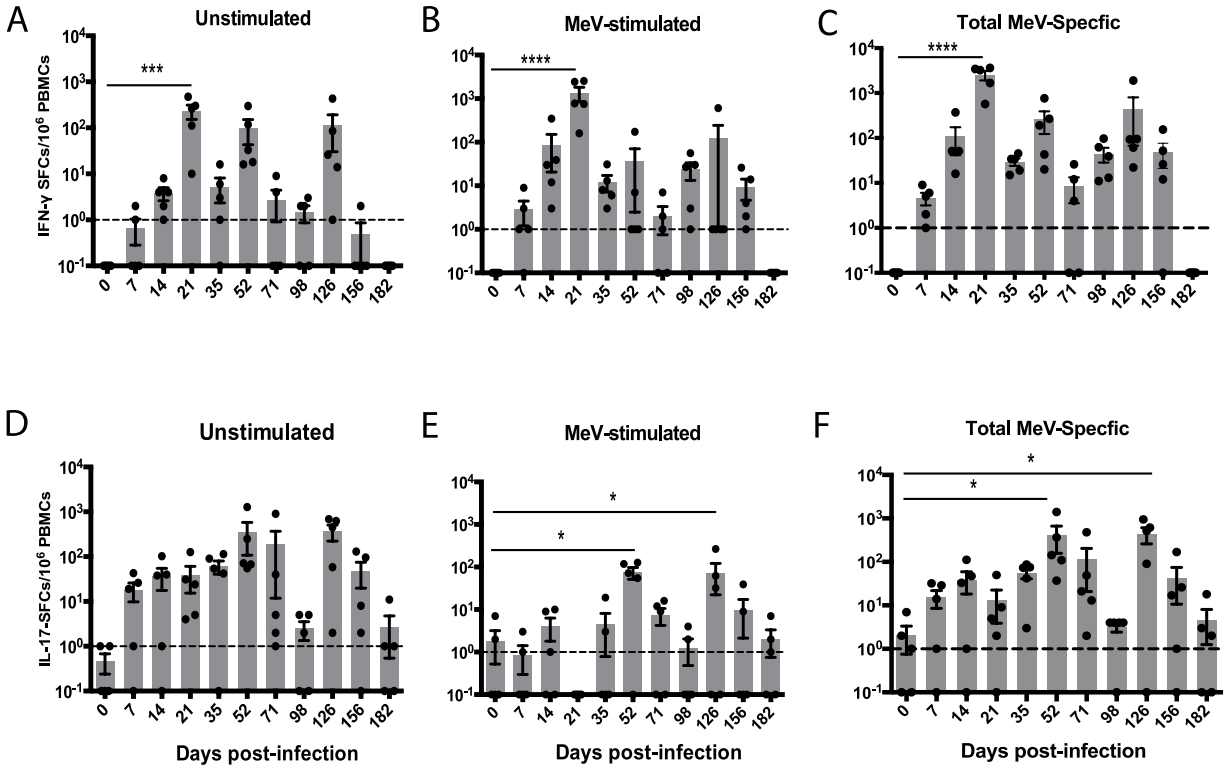

Figure 3. ELISPOT detection of IFN-γ and IL-17-secreting cells. PBMCs from MeV-infected macaques were cultured without *in vitro* stimulation (**A**,D) or were stimulated with H and N peptides (**C**) or MeV lysate (**F**) and cultured on plates coated with antibody to IFN-γ (**A**–**C**) or IL-17A (**D**–**F**) to determine numbers of spot-forming cells (SFCs) per 10^6 PBMCs. To determine the numbers of cells secreting IFN-γ (**B**) or IL-17 (**E**) in response to *in vitro* MeV stimulation, numbers of SFCs in unstimulated wells (**A**,**D**) were subtracted from the numbers of SFCs in MeV H and N (**C**) or MeV lysate (**F**)-stimulated wells. *$P < 0.05$; ***$P < 0.001$; ****$P < 0.0001$. One-way ANOVA with repeated measures followed by Bonferroni multiple comparisons test ($n = 5$).

MeV-specific Tc17 ($CD8^+IL\text{-}17^+$) cells were also induced after MeV infection with patterns of appearance in circulation similar to that of Th17 cells (Fig. 6A,B). All monkeys had an increase in H-specific Tc17 cells to 1.07–1.77% at day 18, whereas only monkey 31Y showed an increase in the frequency of N-specific Tc17 cells at day 18. Monkey 17Y had increases in both H- and N-specific Tc17 cells at day 56, while the other monkeys did not. All monkeys showed an increase in MeV-specific Tc17 cell frequencies at day 168 (Fig. 6B). In summary, MeV H and N-specific $CD4^+$ and $CD8^+$ T cells producing IL-17 were detectable on day 18 when infectious virus was cleared and then again when viral RNA was no longer detectable in PBMCs.

MeV-specific T cell expression of RORγt. To better characterize the IL-17-producing cells, expression of the canonical IL-17 transcription factor RORγt[22] was examined (Fig. 6A–D). The triphasic appearance of MeV-specific Th17 cells was also seen for cells expressing RORγt. All monkeys exhibited an increase in H-specific (1.09% ± 0.23) and N-specific (2.50% ± 1.99) RORγt-expressing $CD4^+$ cells at day 18 (Fig. 6A). Frequencies of RORγt-expressing cells in response to H and N peptide stimulation remained low at day 28 through 39 followed by variable increases at day 56 or day 84. After day 113, the frequencies of MeV-specific RORγt-expressing $CD4^+$ T cells showed a steady increase to approximately 1–2% at day 168 (Fig. 6A).

MeV-specific $CD8^+$ T cells also expressed RORγt (Fig. 6B). Frequencies of H and N-specific $CD8^+ROR\gamma t^+$ T cells were increased at 18, 56 or 64, and 168 days after infection. All monkeys displayed an increase in H-specific RORγt-expressing $CD8^+$ T cells at days 18 and 168 (Fig. 6B). MeV-specific $CD8^+$ T cells expressing RORγt averaged approximately 4% of the total $CD8^+$ T cells, with individual frequencies ranging from 0.5–10%.

In addition, we also characterized the simultaneous expression of IL-17 and RORγt. To better visualize the dynamics of co-expression, histograms of $CD4^+IL\text{-}17^+$ cells and $CD4^+IL\text{-}17^-$ cells (Fig. 6C) and $CD8^+IL\text{-}17^+$ and $CD8^+IL\text{-}17^-$ cells (Fig. 6D) were created and overlaid. Prior to infection, all populations had very low levels of RORγt expression, but by day 18, RORγt expression was detected (Fig. 6C,D). At days 56 and 113, IL-17-positive cells had higher levels of RORγt than IL-17-negative cells in both stimulated and non-stimulated populations. However, at day 168, the *ex vivo* MeV-stimulation does not increase RORγt expression in IL-17-positive relative to IL-17-negative cells.

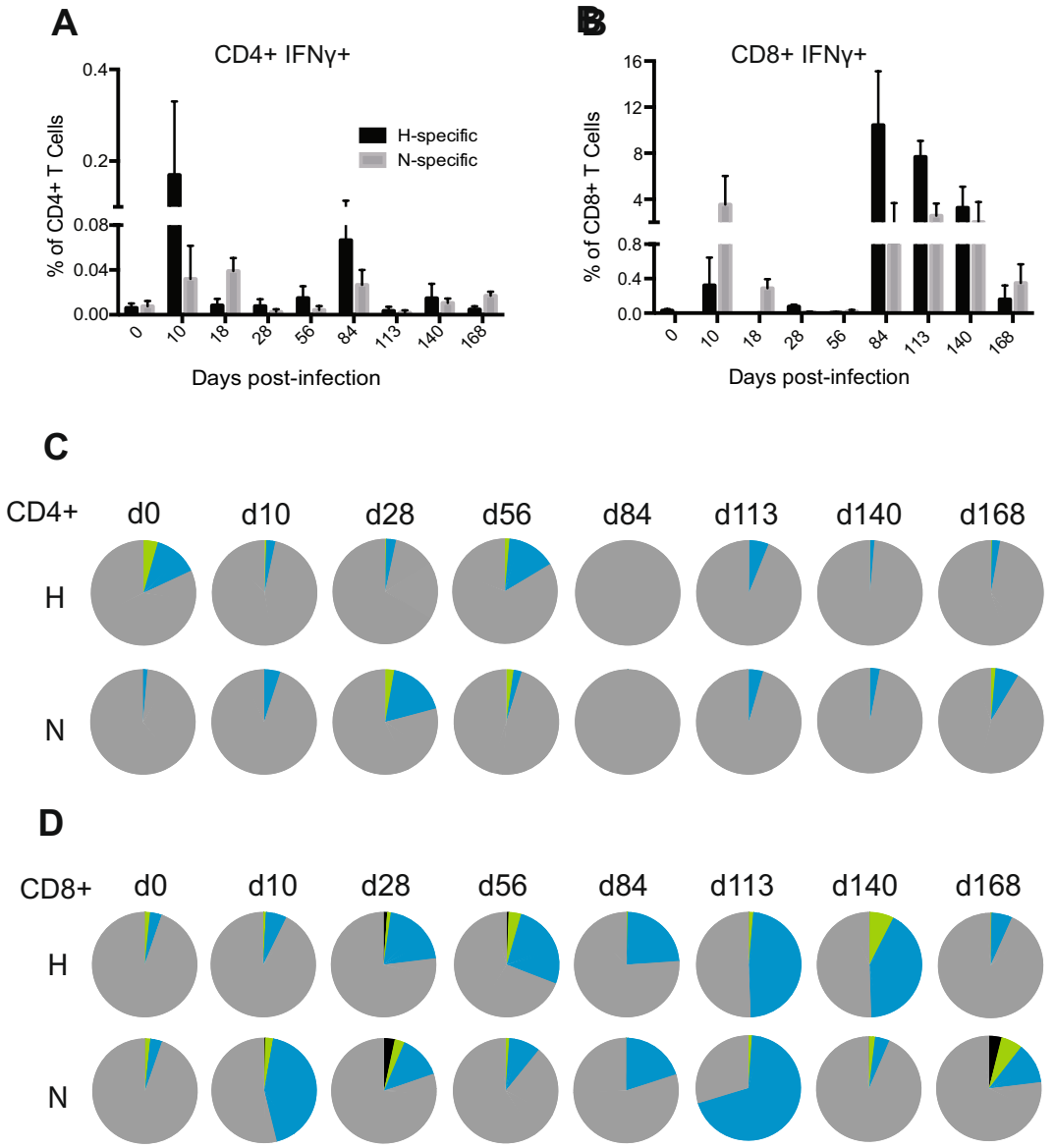

Figure 4. Assessment of the ability of MeV-specific T cells to produce effector cytokines over time by intracellular staining and multicolor flow cytometry. PBMCs were stimulated with pooled overlapping peptides from the MeV H or N proteins and IFN-γ-producing $CD4^+$ cells (**A**) and $CD8^+$ cells (**B**) were identified. The frequency of MeV specific IFN-γ-producing cells was determined by subtracting the spontaneous response. The polyfunctionality of the MeV-specific T cell response was assessed by determining the ability of $CD3^+$ $CD4^+$ cells to simultaneously express IFN-γ, TNFα, or IL-2 (**C**) and $CD3^+$ $CD8^+$ cells for their ability to simultaneously express IFN-γ, CD107a, TNFα, or IL2 (**D**). Pie charts show the functional composition of $CD4^+$ and $CD8^+$ T cells that simultaneously express one (gray), two (blue), three (green), or four (black) different functional markers at a given time point (**C**,**D**) (n = 4–5/time point).

Discussion

Studies of measles in humans and macaques have suggested that T cell responses are important for recovery but the characteristics and time of appearance of MeV-specific T cells has received limited attention[11,23]. In this study, we have monitored the evolution of T cell responses in MeV-infected rhesus macaques for a period of six months. Cells secreting IFN-γ and IL-17 *ex vivo* and responsive to additional *in vitro* MeV stimulation appeared in circulation in multiple waves approximately 2–3, 8 and 18–24 weeks after infection without a change in total lymphocyte counts. IFN-γ-secreting cells entered the circulation within the first 2 weeks and were most abundant 2–3 weeks after infection coincident with clearance of infectious virus. Virus-specific $CD4^+$ (Th1) and $CD8^+$ (Tc1) T cells were sources of IFN-γ early in infection, while $CD8^+$ T cells were the predominant sources of IFN-γ later in infection. IL-17-secreting cells were most abundant later, were both $CD4^+$ (Th17) and $CD8^+$ (Tc17), expressed the transcription factor RORγt and showed specificity for H and N MeV proteins. These data show an ongoing evolution of the virus-specific cellular immune response during MeV clearance and suggest that IFN-γ-production

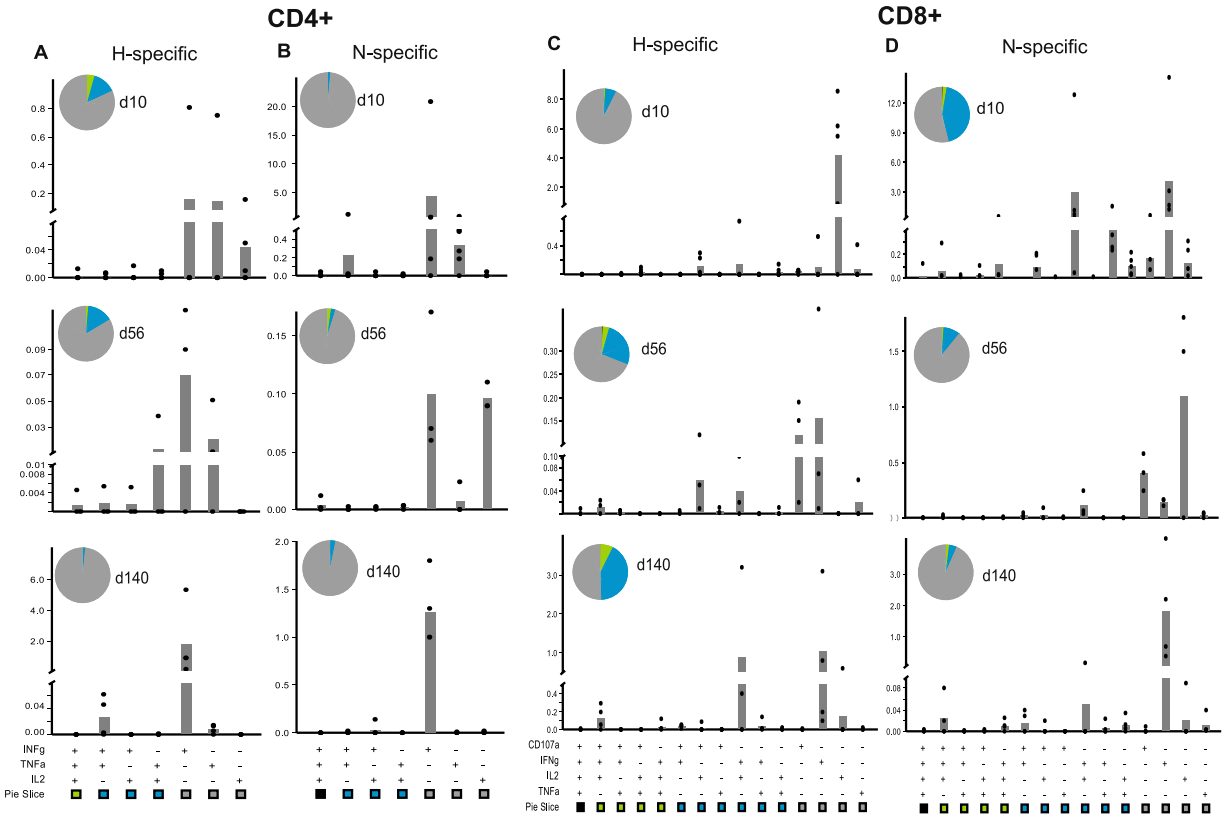

Figure 5. Functional analysis of MeV-specific T cells. PBMCs were stimulated with pooled H and N peptides. $CD3^+CD4^+$ cells were assessed for the ability to simultaneously express IFN-γ, TNFα, or IL-2 (**A** and **B**) and $CD3^+CD8^+$ cells for the ability to simultaneously express IFN-γ, CD107a, TNFα, or IL-2 (**C** and **D**). Subsets of cells expressing each functional marker were analyzed by Boolean gating. The frequency of each subset within $CD4^+$ and $CD8^+$ T cells is shown in the bar chart (n = 4–5/time point).

may be important for early viral control while IL-17 production may be more important late during clearance of viral RNA. Prolonged multi-functional T cell responses may play an important role in maturation of the immune response to measles and establishment of life-long protective immunity.

Many IFN-γ-producing $CD4^+$ and $CD8^+$ cells were polyfunctional, secreting IL-2 and TNF-α as well as IFN-γ. These data are consistent with previous observations of increases in levels of TNFα mRNA in PBMCs and of IFN-γ, soluble IL-2 receptor, soluble CD8 and CD4 in plasma of children at the time of the measles rash[13,14,24–26]. IFN-γ has potent antiviral activities through induction of antiviral proteins and IFN-γ-secreting $CD8^+$ T cells are also likely to have cytotoxic activity, both of which contribute to clearance of many virus infections[27]. *In vivo* depletion of $CD8^+$ T cells has demonstrated their importance for control of measles virus[11], simian immunodeficiency virus (SIV)[28] and hepatitis B virus[29] infections. Furthermore, $CD4^+$ and $CD8^+$ T cells can develop into memory T cells, which are more efficient producers of IFN-γ upon restimulation and provide protection from reinfection. The second increase in IFN-γ^+CD8^+ T cells in response to *ex vivo* stimulation 12–20 weeks after infection may reflect this population. Although more studies are needed to characterize these cells, it is likely that the T cell increase early after infection is important for the clearance of infectious virus while the later response may indicate renewed appearance of effector cells or development of a memory response.

The role(s) of IL-17-producing cells in virus infection are less clear, but they have been implicated in impaired virus clearance and immunopathology, as well as improved outcome[30]. Th17 cells are induced from naïve $CD4^+$ T cells in the presence of IL-6 plus some combination of TGFβ, IL-21 and IL-1β a process that is inhibited by type I IFN[31], and suppresses Foxp3 expression necessary for Treg development. The innate response that occurs after MeV infection may facilitate the development of IL-17-producing cells because IL-6 and IL-1β are increased early, but very little, if any, type I IFN is produced[15,26,32].

The time course for generation of IL-17-producing T cells has not been carefully assessed for most infections; however, a few studies suggest that peak production is often late. For instance, in mice with keratitis due to herpes simplex virus infection, two waves of IL-17 mRNA (d2 and d21) are observed[33]. In children with respiratory syncytial virus-induced bronchiolitis, levels of IL-17 in nasopharyngeal secretions are higher in convalescence than during acute disease, in contrast to the other cytokines and chemokines measured[34]. Previous studies of macaques have shown increases in IL-17-producing cells at 10 and 35 days after MeV infection, but later times were not assessed[16]. In this study we have shown that IL-17-secreting cells were not only produced early in infection (day 18), but also late during the recovery process (day 168) and that both $CD4^+$ and $CD8^+$ T cells are sources of IL-17. It should also be noted that peak IL-17 secretion at 52 days after infection coincides with the reappearance of MeV

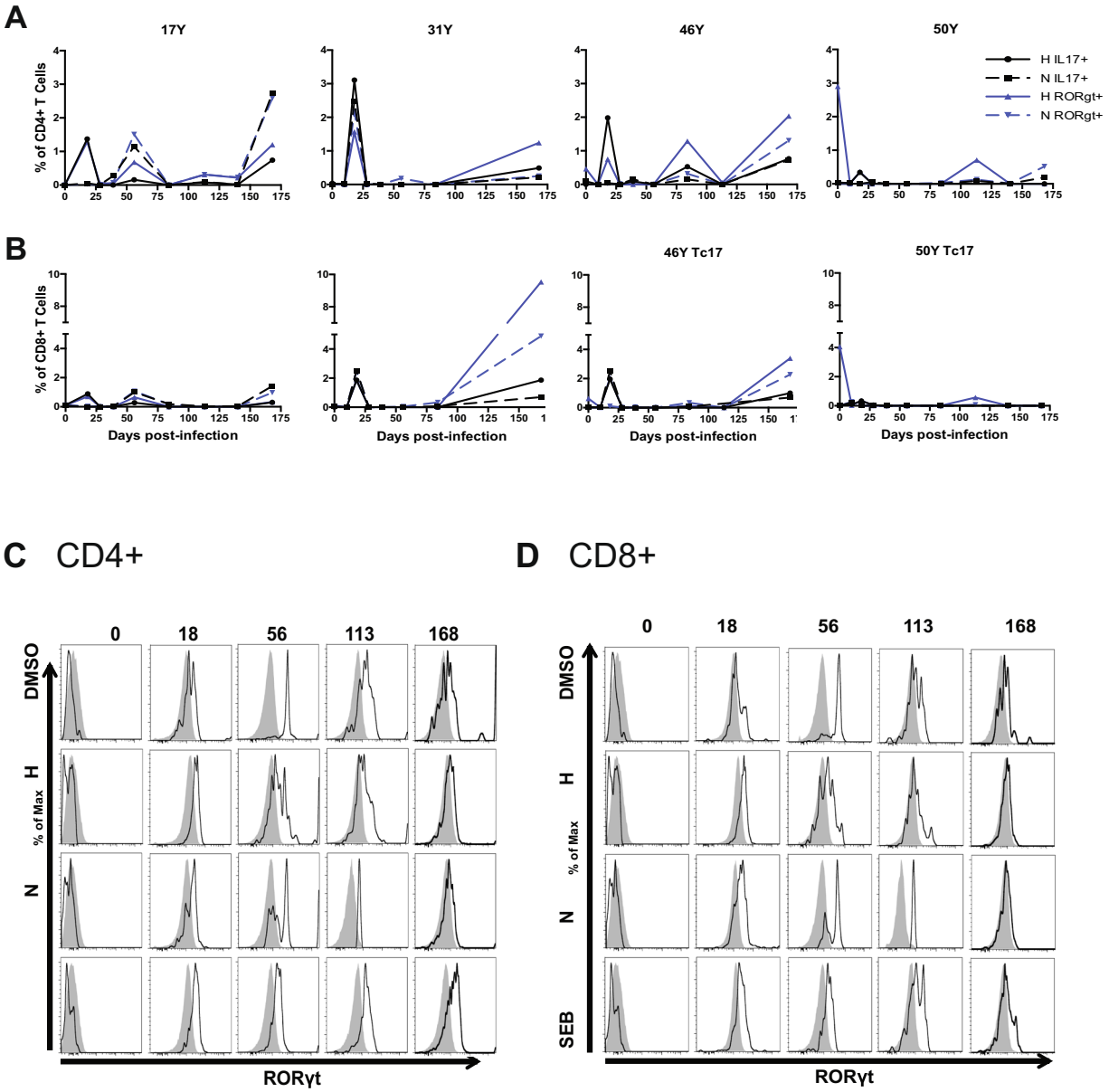

Figure 6. IL-17 and RORγt expression by MeV-specific T cells. PBMCs were stimulated with DMSO diluent, pooled overlapping peptides from the MeV H or N proteins or staphylococcal enterotoxin B (SEB) and IL-17$^+$ and RORγt$^+$ CD4$^+$ (**A**) and CD8$^+$ (**B**) cells were identified by intracellular cytokine staining and multicolor flow cytometry. CD4$^+$IL-17$^+$ (open) and CD4$^+$IL-17$^-$ (gray) populations (**C**), and in CD8$^+$IL-17$^+$ (open) and CD8$^+$IL-17$^-$ (gray) populations (**D**) are overlaid for comparison of RORγt expression.

RNA and is followed by a rapid decrease in viral RNA levels. These data further suggest the possibility that that IL-17 production may promote the clearance of viral RNA. While Th17 cells are polyfunctional, have multiple phenotypes and can play both detrimental and beneficial roles in disease pathogenesis[31,35,36] their role in MeV infections is still unknown.

Virus-specific Th17 cells have been detected as part of the CD4$^+$ T cell response to viral infections of mice[33,37–41], nonhuman primates[42–44] and humans[45–47]. Expression of IL-17 by recombinant vaccinia virus leads to increased levels of virus in tissues[48]. Numbers of NKT cells producing IL-17 correlate with failure to control chronic SIV infection in macaques and higher levels of circulating Th17 cells correlate with higher viral loads and more severe liver disease in humans with chronic hepatitis B virus infection[49]. However, both improved clearance of influenza virus from the lung[50] and no effect on clearance of herpes simplex virus from the cornea[51] are also reported in response to IL-17-producing cells. The mechanism by which IL-17-producing cells may inhibit virus clearance is not clear.

Many innate immune cells including innate lymphoid cells, NK cells, and NKT cells can produce IFN-γ and/or IL-17. It is likely that these cells may contribute to the small burst of IFN-γ and IL-17 detected seven days after infection by ELISPOT assay. However, by 10 days after infection all macaques had developed rash, a hallmark for

the onset of the adaptive immune response during measles infection[1]. Therefore, adaptive immune cells are likely to be the predominant producers of IFN-γ and IL-17 after the first week of infection.

Lastly, measles is associated with a transient period of immune suppression, which may last for several weeks to months after the acute stage of disease. Lymphopenia, a proposed contributor to immune suppression, is observed during the acute phase of infection and is associated with decreased numbers of T cells and B cells in circulation and lymphoid tissue[52]. We observed a transient decrease in T cell numbers at 10 days, which returned to baseline frequencies by 18 days with little variation despite a change in the method for identifying $CD4^+$ T cells by flow cytometry.

These studies highlight the prolonged and complicated cellular immune responses generated by MeV infection. The immunologic processes driving the late development and repeated waves of IFN-γ and IL-17-producing cells and the effects of these responses on MeV RNA clearance are not known and merit further investigation. Although antibody responses were not addressed in this study, it is likely that immune-mediated clearance relies on the development of robust MeV-specific antibody responses as well as effective T cell responses[7].

Methods

Ethics statement. For all procedures, monkeys were sedated with 10–15 mg/kg ketamine intramuscularly. All studies were performed in accordance with experimental protocols approved by the Johns Hopkins University Institutional Animal Care and Use Committee.

Animals, infection and procedures. Five 3-year-old male measles-naïve rhesus macaques (*Macaca mulatta*) were obtained from the Johns Hopkins Primate Breeding Facility. The Bilthoven strain of wild-type MeV (genotype C2; gift of Albert Osterhaus, Erasmus University, Rotterdam) was grown in phytohemagglutinin-stimulated human cord blood cells and assayed by plaque formation on Vero/hSLAM cells[53]. Following baseline measurements, monkeys were infected intratracheally with 10^4 plaque-forming units MeV in 1 ml PBS. Upon development of a rash, monkeys received either two daily doses of vitamin A (100,000 units, Vitamin Angels, Santa Barbara, CA; 14Y, 50Y) or placebo (17Y, 31Y, 46Y). No differences were observed between supplemented and non-supplemented macaques, so data have been pooled. Heparinized blood was collected from the femoral vein before infection and every 3–14 days after infection for six months.

Sample processing and virus quantification. Beginning 10 days after infection, automated complete blood counts were performed by IDEXX Laboratories. PBMCs and plasma were isolated by whole blood gradient centrifugation on Lympholyte-Mammal (Cedarlane Labs). Infectious MeV in blood was measured by co-cultivating serially diluted fresh PBMCs with Vero/hSLAM cells for 5–6 days. Cytopathic effects in each well were assessed and the 50% tissue culture infectious dose ($TCID_{50}$) calculated. Level of viremia is expressed as $TCID_{50}$ per million PBMCs.

MeV RNA in PBMCs was measured by RT-qPCR as previously described[7,54]. Briefly, RNA was isolated from 2×10^6 PBMCs and the nucleocapsid (N) gene was amplified (Applied Biosystems Prism 7700) using a one-step RT-PCR kit with TaqMan primers and probe. Controls included GAPDH amplification and PBMC RNA from MeV-naïve monkeys. Copy number was determined using a standard curve constructed from 10^1–10^8 copies of RNA synthesized by *in vitro* transcription from a plasmid encoding the Edmonston N gene. The sensitivity of the assay was 50–100 copies. Data were normalized to the GAPDH control and expressed as [(copies of MeV N RNA)/(copies of GAPDH RNA)] × 5,000.

Nasal secretions were collected from both nostrils with sterile cotton swabs immersed in PBS. RNA isolated from the nasal cells (RNeasy Plus Micro Kit; Qiagen) was eluted in 30 μl of RNase-free water and 10 ng or 10 μl was used for RT-PCR. Primers MV41 (5′CATTACATCAGGATCCGG-3′) and MV42 (5′-GTATTGGTCCGCCTCATC-3′) were used to amplify a 350 base pair N gene sequence, and human β-actin RT-PCR primers (Agilent) were used as a control for RNA quality. PCR products were run on gels and read as positive or negative.

ELISPOT assays. Enzyme-linked immunosorbent spot (ELISPOT) assays were used to identify PBMCs secreting IFN-γ and IL-17. Multiscreen HTS HA Opaque 96-well filtration plates (Millipore) were coated with mouse anti-human IFN-γ antibody (BD Biosciences, 2 μg/ml) or IL-17A antibody (eBioscience, 5 μg/ml) and blocked with RPMI/10% FBS. Cells were not stimulated or were stimulated with 1 μg/ml pooled hemagglutinin (H) or N overlapping peptides, 5.8 μg/ml MeV-infected Vero cell lysate (Advanced Biotechnologies) or 5 μg/ml concanavalin A. Freshly isolated PBMCs (10^5) were added to wells stimulated with ConA, H or N peptides and 5×10^5 PBMCs were added to non-stimulated and MeV lysate wells and incubated at 37 °C/5%CO_2 for 40–42 h. Biotinylated anti-human IFN-γ (Mabtech, 7-B6-1; 1 μg/ml) or anti-human IL-17A (eBioscience, 64DEC17; 2 μg/ml) antibody was added for 2 h. Plates were developed with avidin-horseradish peroxidase (BD Biosciences; 1:2000) and diaminobenzidine substrate. Plates were read and analyzed using an ImmunoSpot plate reader and ImmunoSpot 5.0 software (C.T.L.). Data are presented as total spot-forming cells (SFCs)/10^6 PBMCs. MeV-specific SFCs stimulated to secrete cytokines *ex vivo* were determined by subtracting the *in vivo* activated (no *in vitro* stimulation) SFCs from the total SFCs at each time point. All assays were done in duplicate.

Flow cytometry. Multicolor flow cytometry with intracellular cytokine staining was used to identify $CD4^+$ and $CD8^+$ T cells expressing IFN-γ, IL-17, and RORγt. PBMCs were stimulated for 12 h using pooled overlapping H or N peptides (1 μg/ml), peptide diluent dimethyl sulfoxide (DMSO) or staphylococcal enterotoxin B. Except where noted, all reagents were from BD Biosciences or eBioscience. Mouse anti-human CD28 (CD28.2) and anti-human CD49d (9F10) were included with the peptides and DMSO. All stimulation mixes included GolgiStop and GolgiPlug.

Live/Dead Fixable Violet Dead Cell Stain Kit (Invitrogen) was used to eliminate dead cells from the analysis. Prior to surface staining, cells were incubated with human FcR block. All panels included anti-CD3 antibody (SP34-2). For days 0–18 a "dump gate" was used to eliminate cells labeled with anti-human CD14 (M5E2), anti-human CD20 (2H7) or anti-human CD8 (SK1) and $CD4^+$ cells were defined as $CD14^-CD20^-CD3^+CD8^-$, because the anti-CD4 antibody initially used (RPA-T4) stained monkey $CD4^+$ T cells poorly. From day 28 onward, anti-human CD4 (Biolegend, OKT4) was used and $CD4^+$ T cells were defined as $CD14^-CD20^-CD3^+CD4^+$. $CD8^+$ cells were defined as $CD14^-CD20^-CD3^+CD8^+$.

Intracellular staining was done following fixation and permeabilization of cells. For days 7–21 the Cytofix/Cytoperm Fixation and Permeabilization Kit and subsequently the Foxp3 Staining Buffer Set was used. Intracellular staining was done to detect the transcription factor RORγt (Q21-559) and the cytokines IFN-γ and IL-1-. T cell functionality was determined by gating on $CD3^+CD4^+$ and $CD3^+CD8^+$ cells stained for expression of IFN-γ, tumor necrosis factor alpha (TNFα), IL-2 or CD107a. Boolean gating was used to define all possible subsets. Percentages of cells that expressed one, two, three or four different functional markers were grouped and relative frequencies for each subset within $CD3^+CD4^+$ and $CD3^+CD8^+$ T cell populations were calculated. Samples were run on a BD FACS Canto II flow cytometer and analyzed using BD FACSDiva, FlowJo and SPICE (version 5.1; NIAID, NIH) software.

Statistical analysis. The significance of differences in IFN-γ and IL-17-secreting cells was assessed by a one-way ANOVA with repeated measures followed by Bonferroni's multiple comparisons test (GraphPad Prism version 7.00). Means for each time point were compared to the day 0 pre-infection levels. A p-value < 0.05 was considered significant.

References

1. Moss, W. J. & Griffin, D. E. Measles. *Lancet* **379**, 153–164, doi:10.1016/S0140-6736(10)62352-5 (2012).
2. Beckford, A. P., Kaschula, R. O. & Stephen, C. Factors associated with fatal cases of measles. A retrospective autopsy study. *South Afr. Med. J.* **68**, 858–863 (1985).
3. Miller, D. L. Frequency of complications of measles, 1963. *Brit. Med. J.* **2**, 75–78 (1964).
4. Polack, F. P. *et al*. Production of atypical measles in rhesus macaques: evidence for disease mediated by immune complex formation and eosinophils in the presence of fusion-inhibiting antibody. *Nature Med.* **5**, 629–634, doi:10.1038/9473 (1999).
5. Permar, S. R. *et al*. Prolonged measles virus shedding in human immunodeficiency virus-infected children, detected by reverse transcriptase-polymerase chain reaction. *J. Infect. Dis.* **183**, 532–538, doi:10.1086/318533 (2001).
6. Riddell, M. A., Moss, W. J., Hauer, D., Monze, M. & Griffin, D. E. Slow clearance of measles virus RNA after acute infection. *J. Clin. Virol.* **39**, 312–317, doi:10.1016/j.jcv.2007.05.006 (2007).
7. Lin, W. H., Kouyos, R. D., Adams, R. J., Grenfell, B. T. & Griffin, D. E. Prolonged persistence of measles virus RNA is characteristic of primary infection dynamics. *Proc. Natl. Acad. Sci. USA* **109**, 14989–14994, doi:10.1073/pnas.1211138109 (2012).
8. Kaplan, L. J., Daum, R. S., Smaron, M. & McCarthy, C. A. Severe measles in immunocompromised patients. *JAMA* **267**, 1237–1241 (1992).
9. Permar, S. R., Griffin, D. E. & Letvin, N. L. Immune containment and consequences of measles virus infection in healthy and immunocompromised individuals. *Clin. Vaccine Immunol.* **13**, 437–443, doi:10.1128/CVI.13.4.437-443.2006 (2006).
10. Jaye, A., Magnusen, A. F., Sadiq, A. D., Corrah, T. & Whittle, H. C. *Ex vivo* analysis of cytotoxic T lymphocytes to measles antigens during infection and after vaccination in Gambian children. *J. Clin. Invest.* **102**, 1969–1977, doi:10.1172/JCI3290 (1998).
11. Permar, S. R. *et al*. Role of CD8(+) lymphocytes in control and clearance of measles virus infection of rhesus monkeys. *J. Virol.* **77**, 4396–4400 (2003).
12. Nakayamada, S., Takahashi, H., Kanno, Y. & O'Shea, J. J. Helper T cell diversity and plasticity. *Curr. Opin. Immunol.* **24**, 297–302, doi:10.1016/j.coi.2012.01.014 (2012).
13. Griffin, D. E. & Ward, B. J. Differential CD4 T cell activation in measles. *J. Infect. Dis.* **168**, 275–281 (1993).
14. Moss, W. J., Ryon, J. J., Monze, M. & Griffin, D. E. Differential regulation of interleukin (IL)-4, IL-5, and IL-10 during measles in Zambian children. *J. Infect. Dis.* **186**, 879–887, doi:10.1086/344230 (2002).
15. Lin, W. W., Nelson, A., Ryon, J. J., Moss, W. J. & Griffin, D. E. Plasma cytokines and chemokines in Zambian children with measles: innate responses and association with HIV-1 co-infection and in-hospital mortality. *J. Infect. Dis.*. doi:10.1093/infdis/jix012 (2017).
16. Lin, W. H. *et al*. Vaxfectin adjuvant improves antibody responses of juvenile rhesus macaques to a DNA vaccine encoding the measles virus hemagglutinin and fusion proteins. *J. Virol.* **87**, 6560–6568, doi:10.1128/JVI.00635-13 (2013).
17. Pantaleo, G. & Harari, A. Functional signatures in antiviral T-cell immunity for monitoring virus-associated diseases. *Nature Rev. Immunol.* **6**, 417–423, doi:10.1038/nri1840 (2006).
18. Kannanganat, S., Ibegbu, C., Chennareddi, L., Robinson, H. L. & Amara, R. R. Multiple-cytokine-producing antiviral CD4 T cells are functionally superior to single-cytokine-producing cells. *J. Virol.* **81**, 8468–8476, doi:10.1128/JVI.00228-07 (2007).
19. Kannanganat, S. *et al*. Human immunodeficiency virus type 1 controllers but not noncontrollers maintain CD4 T cells coexpressing three cytokines. *J. Virol.* **81**, 12071–12076, doi:10.1128/JVI.01261-07 (2007).
20. Gibson, L. *et al*. Reduced frequencies of polyfunctional CMV-specific T cell responses in infants with congenital CMV infection. *J. Clin. Immunol.* **35**, 289–301, doi:10.1007/s10875-015-0139-3 (2015).
21. Han, Q. *et al*. Polyfunctional responses by human T cells result from sequential release of cytokines. *Proc. Natl. Acad. Sci. USA* **109**, 1607–1612, doi:10.1073/pnas.1117194109 (2012).
22. Ivanov, I. I. *et al*. The orphan nuclear receptor RORgammat directs the differentiation program of proinflammatory IL-17 + T helper cells. *Cell* **126**, 1121–1133, doi:10.1016/j.cell.2006.07.035 (2006).
23. Lin, W. H., Pan, C. H., Adams, R. J., Laube, B. L. & Griffin, D. E. Vaccine-induced measles virus-specific T cells do not prevent infection or disease but facilitate subsequent clearance of viral RNA. *mBio* **5**, e01047, doi:10.1128/mBio.01047-14 (2014).
24. Griffin, D. E., Ward, B. J., Jauregui, E., Johnson, R. T. & Vaisberg, A. Immune activation in measles. *New Engl. J. Med.* **320**, 1667–1672, doi:10.1056/NEJM198906223202506 (1989).
25. Griffin, D. E., Ward, B. J., Jauregui, E., Johnson, R. T. & Vaisberg, A. Immune activation during measles: interferon-gamma and neopterin in plasma and cerebrospinal fluid in complicated and uncomplicated disease. *J. Infect. Dis.* **161**, 449–453 (1990).
26. Zilliox, M. J., Moss, W. J. & Griffin, D. E. Gene expression changes in peripheral blood mononuclear cells during measles virus infection. *Clin. Vaccine Immunol.* **14**, 918–923, doi:10.1128/CVI.00031-07 (2007).
27. Binder, G. K. & Griffin, D. E. Interferon-gamma-mediated site-specific clearance of alphavirus from CNS neurons. *Science* **293**, 303–306, doi:10.1126/science.1059742 (2001).
28. Schmitz, J. E. *et al*. Control of viremia in simian immunodeficiency virus infection by CD8 + lymphocytes. *Science* **283**, 857–860 (1999).

29. Thimme, R. *et al.* CD8(+) T cells mediate viral clearance and disease pathogenesis during acute hepatitis B virus infection. *J. Virol.* **77**, 68–76 (2003).
30. Swain, S. L., McKinstry, K. K. & Strutt, T. M. Expanding roles for CD4(+) T cells in immunity to viruses. *Nature Rev. Immunol.* **12**, 136–148, doi:10.1038/nri3152 (2012).
31. Korn, T., Bettelli, E., Oukka, M. & Kuchroo, V. K. IL-17 and Th17 Cells. *Annu. Rev. Immunol.* **27**, 485–517, doi:10.1146/annurev.immunol.021908.132710 (2009).
32. Shivakoti, R. *et al.* Limited *in vivo* production of type I or type III interferon after infection of macaques with vaccine or wild-type strains of measles virus. *J. Interferon & Cytokine Res.* **35**, 292–301, doi:10.1089/jir.2014.0122 (2015).
33. Suryawanshi, A. *et al.* Role of IL-17 and Th17 cells in herpes simplex virus-induced corneal immunopathology. *J. Immunol.* **187**, 1919–1930, doi:10.4049/jimmunol.1100736 (2011).
34. Faber, T. E., Groen, H., Welfing, M., Jansen, K. J. & Bont, L. J. Specific increase in local IL-17 production during recovery from primary RSV bronchiolitis. *J. Med. Virol.* **84**, 1084–1088, doi:10.1002/jmv.23291 (2012).
35. Peters, A., Lee, Y. & Kuchroo, V. K. The many faces of Th17 cells. *Curr. Opin. Immunol.* **23**, 702–706, doi:10.1016/j.coi.2011.08.007 (2011).
36. Onishi, R. M. & Gaffen, S. L. Interleukin-17 and its target genes: mechanisms of interleukin-17 function in disease. *Immunology* **129**, 311–321, doi:10.1111/j.1365-2567.2009.03240.x (2010).
37. Arens, R. *et al.* Cutting edge: murine cytomegalovirus induces a polyfunctional CD4 T cell response. *J. Immunol.* **180**, 6472–6476 (2008).
38. Hou, W., Kang, H. S. & Kim, B. S. Th17 cells enhance viral persistence and inhibit T cell cytotoxicity in a model of chronic virus infection. *J. Exp. Med.* **206**, 313–328, doi:10.1084/jem.20082030 (2009).
39. Li, C. *et al.* IL-17 response mediates acute lung injury induced by the 2009 pandemic influenza A (H1N1) virus. *Cell Res.* **22**, 528–538, doi:10.1038/cr.2011.165 (2012).
40. Xie, Y. *et al.* The role of Th17 cells and regulatory T cells in Coxsackievirus B3-induced myocarditis. *Virology* **421**, 78–84, doi:10.1016/j.virol.2011.09.006 (2011).
41. Crowe, C. R. *et al.* Critical role of IL-17RA in immunopathology of influenza infection. *J. Immunol.* **183**, 5301–5310, doi:10.4049/jimmunol.0900995 (2009).
42. Campillo-Gimenez, L. *et al.* AIDS progression is associated with the emergence of IL-17-producing cells early after simian immunodeficiency virus infection. *J. Immunol.* **184**, 984–992, doi:10.4049/jimmunol.0902316 (2010).
43. Cecchinato, V. & Franchini, G. Th17 cells in pathogenic simian immunodeficiency virus infection of macaques. *Curr. Opin. HIV AIDS* **5**, 141–145, doi:10.1097/COH.0b013e32833653ec (2010).
44. Khowawisetsut, L. *et al.* Relationships between IL-17(+) subsets, Tregs and pDCs that distinguish among SIV infected elite controllers, low, medium and high viral load rhesus macaques. *PloS One* **8**, e61264, doi:10.1371/journal.pone.0061264 (2013).
45. Yue, F. Y. *et al.* Virus-specific interleukin-17-producing CD4+ T cells are detectable in early human immunodeficiency virus type 1 infection. *J. Virol.* **82**, 6767–6771, doi:10.1128/JVI.02550-07 (2008).
46. Basha, H. I. *et al.* Characterization of HCV-specific CD4+ Th17 immunity in recurrent hepatitis C-induced liver allograft fibrosis. *Am. J. Transplan.* **11**, 775–785, doi:10.1111/j.1600-6143.2011.03458.x (2011).
47. Li, S. *et al.* Peripheral T lymphocyte subset imbalances in children with enterovirus 71-induced hand, foot and mouth disease. *Virus Res.* **180**, 84–91, doi:10.1016/j.virusres.2013.11.021 (2014).
48. Patera, A. C., Pesnicak, L., Bertin, J. & Cohen, J. I. Interleukin 17 modulates the immune response to vaccinia virus infection. *Virology* **299**, 56–63 (2002).
49. Zhang, J. Y. *et al.* Interleukin-17-producing CD4(+) T cells increase with severity of liver damage in patients with chronic hepatitis B. *Hepatology* **51**, 81–91, doi:10.1002/hep.23273 (2010).
50. McKinstry, K. K. *et al.* Memory CD4+ T cells protect against influenza through multiple synergizing mechanisms. *J. Clin. Invest.* **122**, 2847–2856, doi:10.1172/JCI63689 (2012).
51. Molesworth-Kenyon, S. J., Yin, R., Oakes, J. E. & Lausch, R. N. IL-17 receptor signaling influences virus-induced corneal inflammation. *J. Leuk. Biol.* **83**, 401–408, doi:10.1189/jlb.0807571 (2008).
52. Ryon, J. J., Moss, W. J., Monze, M. & Griffin, D. E. Functional and phenotypic changes in circulating lymphocytes from hospitalized Zambian children with measles. *Clin. Diag. Lab. Immunol.* **9**, 994–1003 (2002).
53. Ono, N. *et al.* Measles viruses on throat swabs from measles patients use signaling lymphocytic activation molecule (CDw150) but not CD46 as a cellular receptor. *J. Virol.* **75**, 4399–4401, doi:10.1128/JVI.75.9.4399-4401.2001 (2001).
54. Pan, C. H. *et al.* Modulation of disease, T cell responses, and measles virus clearance in monkeys vaccinated with H-encoding alphavirus replicon particles. *Proc. Natl. Acad. Sci. USA* **102**, 11581–11588, doi:10.1073/pnas.0504592102 (2005).

Acknowledgements

This work was supported by grants from the National Institutes of Health (R21 AI095981to D.E.G., T32 OD011089 to V.K.B. and T32 AI007417 to A.N.N.), and by a scholarship from the Wisconsin Chapter of the Metals Service Center Institute to N.P. We thank Wen-Hsuan Lin for preparation of the stock Bilthoven MeV used for infection and for helpful advice on analysis of immune responses in macaques.

Author Contributions

A.N.N., N.P. and D.E.G. designed experiments; A.N.N., N.P., D.H., V.K.B. and R.J.A. performed. experiments; A.N.N., N.P. and D.E.G. interpreted data; A.N.N., N.P. and D.E.G. wrote manuscript.

Additional Information

Competing Interests: The authors declare that they have no competing interests.

Publisher's note: Springer Nature remains neutral with regard to jurisdictional claims in published maps and institutional affiliations.